CARBON 50 (2012) 1447–1454

Available at www.sciencedirect.com

SciVerse ScienceDirect

journal homepage: www.elsevier.com/locate/carbon

Increased response/recovery lifetimes and reinforcement of polyaniline nanofiber films using carbon nanotubes

Fiona M. Blighe [a,c,*], *Dermot Diamond* [a], *Jonathan N. Coleman* [b,c], *Emer Lahiff* [a]

[a] *CLARITY Centre for Web Technologies, National Centre for Sensor Research (NSCR), Dublin City University, Dublin 9, Ireland*
[b] *Centre for Research on Adaptive Nanostructures and Nanodevices (CRANN), Trinity College Dublin, Dublin 2, Ireland*
[c] *School of Physics, Trinity College Dublin, Dublin 2, Ireland*

ARTICLE INFO

Article history:
Received 8 February 2011
Accepted 11 October 2011
Available online 19 October 2011

ABSTRACT

We have prepared high surface area, conductive, mechanically robust, responsive polyaniline–carbon nanotube composite films. These were produced by filtration from dilute dispersions of polyaniline nanofibers and single-walled carbon nanotubes. Unlike polyaniline alone, these composites are mechanically stable, maintain large intractable surfaces and exhibit greatly enhanced response/recovery behavior to changes in their local environment. This is illustrated by exposing the films to ammonia.

1. Introduction

Currently there is much interest in the area of 'wireless sensor networks' [1]. The concept behind such research envisages a situation whereby the status of the real world is monitored by large numbers of distributed sensors that continuously feedback data which is analyzed, has the relevant information extracted and initiates the appropriate response. Many requirements must be fulfilled before such systems can be realized, including low power usage, low cost and self-sustainability over extended periods of time. Many chemo-/biosensors are prone to degradation. They depend on responsive materials and surfaces to interact with their chosen target and must regularly be calibrated or replaced to compensate for changes in their operating characteristics over time. The development of responsive materials that are stable and continue to respond and recover after repeated exposure to a target is one of the key roles of material science in facilitating the development of "wireless sensor networks".

A variety of conducting polymers have been suggested as active, responsive components in sensors as they possess good electrical conductivity along with low density and processability [2]. Polyaniline (PAni) is an example of a well-studied conducting polymer which has been investigated for a diverse range of applications [3–7] including as the active material for biological and chemical sensing applications [8–11]. PAni can be chemically (or electrochemically) switched reversibly between two or more redox states [12]. Each state has its own distinct electrical, electrochemical and optical characteristics.

Conductivity occurs in PAni through doping, protons attach to the PAni backbone resulting in bipolaron formation, and this enables charge transfer along the polymer. In the presence of a base the opposite occurs, PAni deprotonates switching rapidly to its non-conductive (dedoped) form. Typically, the conductivity of PAni is not stable over long periods of time due to dopant leaching [13], where small molecular dopants like HCl can dissolve in residual water and subsequently be lost through evaporation [14] this is especially relevant in ambient environments and results in the failure of the PAni to respond to a target. This restricts the use of PAni for applications where extended response/recovery capabilities are required.

Self-sustainability is a prerequisite if PAni is to be considered suitable as the active material in future autonomous sensors. A report by Crowley et al. looks at stability in inkjet

* *Corresponding author at:* CLARITY Centre for Web Technologies, National Centre for Sensor Research (NSCR), Dublin City University, Dublin 9, Ireland. Fax: +353 1 7007995.
E-mail address: Fiona.blighe@dcu.ie (F.M. Blighe).
0008-6223/$ - see front matter
doi:10.1016/j.carbon.2011.10.022

printed PAni nanoparticle electrodes for ammonia detection. They report a stable response over 15 days [15]. Testing however was done using a flow injection system for aqueous ammonia, with samples injected daily in triplicate (so a total of 45 cycles), thus preventing PAni from drying out and avoiding the problem of dopant loss through evaporation. In another example, Wang et al. fabricated polyaniline resistive sensors [10]. These sensors respond to 0.5 ppm ammonia; however the response signal degraded noticeably over 1400 s (23 min) of testing.

The surface to volume ratio of a material is an important property for active sensing materials as increasing this ratio can lead to dramatic enhancement of sensor sensitivity and response time [16–20]. Recently, interest has developed in the nanofiber form of polyaniline [21,22]. PAni nanofibers are pseudo one-dimensional objects that are 30–50 nm in diameter and up to several microns in length [16]. They combine the advantages of an organic conductor with those of a high surface area nano-material.

In addition to issues with extended response/recovery capabilities the promise of PAni is also hampered by poor mechanical properties [23]. PAni tends to be a brittle material with poor ductility. Although films of PAni nanofibers can be cast onto many substrates [22], it is not possible to produce films which are mechanically robust enough to be free-standing. PAni nanofibers have essentially no bulk strength as they do not bind together like the chains in a regular bulk polymer, in fact their attraction to each other is so weak they can be easily dispersed in slightly acidic water [24].

The main advantage of PAni nanofibers over bulk PAni is their increased surface area, which facilitates efficient ion diffusion. Any attempt at preparing PAni nanofiber composites must ensure the nanofibers large surface area is preserved. With this in mind a novel approach must be taken to reinforce and extend the responsive lifetime of the PAni nanofibers, while simultaneously retaining their high surface area. Here we describe how this can be achieved by incorporating carbon nanotubes.

Carbon nanotubes (CNTs) are an allotrope of carbon with a cylindrical nanostructure that possess superlative thermal, electrical and mechanical properties [25,26]. There has been considerable research interest and many suggested applications for CNTs which include conductive and high-strength composites, energy storage/conversion devices and sensors [27,28]. Perhaps one of the most significant properties of CNTs is their large aspect ratio, which is often greater than a thousand. This anisotropy, coupled with excellent mechanical properties, makes nanotubes especially suitable for the mechanical reinforcement of polymers [26]. Much of the research on polymer reinforcement using CNTs has focused on taking a relatively strong material like a bulk thermoplastic polymer and creating an even stronger one by adding a small amount of CNTs as the filler [26,29]. In such composites the weaker polymer acts as a matrix containing the stronger reinforcing agent, namely CNTs.

CNTs have previously been combined with both bulk and nano PAni to improve its properties for a range of applications, including actuation and sensing [4,6,30–40]. For example, Spinks et al. report using CNTs to improve the tensile strength and stress loading of PAni for artificial muscles [6]. Fibers were made by wet spinning whereby bulk PAni powder was added to a CNT acid dispersion. The resulting composite fibers were ~100 μm in diameter. In another example, aniline can be polymerized in the presence of MWNTs to produce a composite powder which, in the dedoped state, can be dissolved and cast onto substrates [41]. Yan et al. prepared nanostructured PAni–CNT composites from colloidal dispersions of acid functionalized MWNTs with PAni nanofibers [42]. The CNT–PAni nanofiber composite precipitates out over time and is held together by electrostatic interactions between the positively charged PAni nanofibers and negatively charged MWNTs. Using this method, the composite produced is a brittle powder. In the only other example of a free-standing high surface area film that the authors are aware of, CNT bucky paper films are made and the aniline monomer is subsequently polymerized over the CNT network to produce a PAni coating onto the CNTs [43]. This results in a paper structure which is 70% porous – thus ensuring a high surface area and impressive capacitance (424 F g^{-1}). The authors also prepared a powder composite by dispersing MWNTs in aniline and subsequent polymerization. This results in a nanostructured material which, while porous, is very brittle when cast as a solid. None of the aforementioned articles however, investigated the effect of the presence of CNTs on the responsive lifetime of PAni.

In this paper we address the two main limitations of PAni nanofibers; namely their lack of mechanical strength and their relatively short response/recovery lifetimes. We demonstrate how significant improvements can be achieved using CNTs to provide a mechanical supportive scaffold and to extend the response/recovery lifetime of PAni nanofibers.

The method we used is analogous to making CNT bucky papers. Bucky papers are macroscopic structures of CNTs where bundles of nanotubes are arranged in a porous mesh held together by van der Waals interactions between neighboring bundles [27]. They are of interest as they are highly porous structures with high surface areas. CNT bucky papers are low density, highly conductive and possess reasonable mechanical properties. Typical conductivities lie between 100 S/m and 10^4 S/m, with densities in the region of 400 kg/m^3 and strengths of 5–10 MPa [27]. Previous research has used bucky papers as a scaffold to contain bulk polymers such as polystyrene, increasing their conductivity and mechanical properties [44,45]. Here we report, for the first time, the preparation of PAni nanofiber–CNT composite buckypapers from stable nano-dispersions of known concentration. The resulting composite films are nanoporous, stable and free-standing with average densities of 510 kg/m^3. We demonstrate how, unlike PAni alone, they display a continuous response/recovery to a target gas and suggest that they may have future application as the active component in autonomous sensors.

2. Experimental

2.1. PAni nanofiber synthesis

Aniline (BDH), HCl (Fisher Scientific), and ammonium peroxydisulfate (Aldrich) were used. The aniline monomer was purified by vacuum distillation before use. Purified aniline was stored under nitrogen in a sealed container at 4 °C. Other

chemicals were used as received. Polyaniline nanofibers were synthesized under ambient conditions by interfacial polymerization between an aqueous and an organic layer [21]. The aqueous layer contained hydrochloric acid (1 M HCl) as the dopant acid and ammonium peroxydisulfate (60 mmol, $(NH_4)2S_2O_8$) as the oxidizing agent. The organic layer contained purified aniline (200 mmol, $C_6H_5NH_2$) dissolved in toluene. Green polyaniline appeared initially at the interface and then migrated into the aqueous phase, after 24 h the reaction was complete. The product was purified by centrifugation (3000 rpm/10 min/3 cycles) and suspended as a colloid in deionized water.

2.2. SWNT dispersions

Purified SWNTs (HiPCO) and the surfactant sodium dodecyl sulfate (SDS) (Aldrich) were used as received. Dispersions were prepared by adding SWNTs (0.35 mg ml^{-1}) to solutions of sodium dodecyl sulfate (SDS, Aldrich) in demonized water (0.44 mg ml^{-1}) and sonicating for 5 min using a high-power ultrasonic tip (GEX600, 120 W, 60 kHz). To achieve a nanotube concentration of 0.0875 mg ml^{-1}, the initial dispersion was diluted twice with surfactant solution, sonicating for 1 min between steps. The diluted dispersions underwent a further 1 h sonication in a low-power ultrasonic bath followed by 5 min under the sonic tip. All dispersions were subsequently centrifuged at 5500 rpm for 90 min to remove any large aggregates. UV–vis absorption measurements were made using a Perkin-Elmer Lambda 900 UV–vis–NIR spectrometer to find the concentration of the nanotube dispersions.

2.3. Composites

A well-known problem with PAni is that it is insoluble in almost all solvents (with the exception of NMP), thus making it difficult to process. Bulk PAni particles are known to agglomerate resulting in poor quality dispersions. A major advantage of the nanofiber form of PAni is that it forms stable aqueous colloidal dispersions. This can be achieved at a pH of around 2.6 without surfactants [46].

The quality of any composite film prepared from dispersion is very much dependent on the quality of the starting dispersion. It has been reported that poor nanotube dispersions produce weak composites, as CNTs form bundles which slip easily over each other leading to defects [29]. Fortunately CNTs are known to disperse well using certain amide solvents [47] and surfactants at near neutral pHs [48]. The mechanism for stabilization of carbon nanotubes by ionic surfactants, like sodium dodecylsulfate, is electrostatic repulsion (as characterized by the zeta potential) [49].

In order to combine CNT and PAni nanofiber dispersions into a stable composite dispersion that does not aggregate prematurely, the pH of the NT dispersion needs to be adjusted using dilute hydrochloric acid. Zeta potential measurements of CNTs dispersed in SDS, measured as a function of pH, show zeta potential values consistent with stable dispersions at all pH values measured [50]. Stable composite dispersions could therefore be made at pH 2.6.

While preparing both PAni and CNT dispersions, their concentration, compatibility and stability had to be considered. Concentrations were calculated using the Beer–Lambert law ($A = \varepsilon Cl$, where A is absorbance, ε the extinction coefficient, and l the path length of the cuvette). The extinction coefficient for CNTs is well known [51]. We calculated the extinction coefficient for PAni nanofibers, in a similar manner, to be 835 (±2) at 529 nm.

Dispersions of both the PAni wires and the SWNTs were combined and sonicated together in a low-power ultrasonic bath for 20 min before being vacuum filtered through a Teflon filter paper (pore size = 0.45 μm), they were then washed with demonized water and dried at ambient temperature for 12 h in a vacuum oven. After drying the films were easily removed from the filter paper. The composites contained equal masses of PAni nanofibers and SWNTs. Reference films of only CNTs were also prepared, along with filter paper supported films of PAni nanofibers. The PAni nanofiber films could not be made to be either free standing, or of a thickness >5 μm, due to cracking, Fig. 1.

2.4. Composite characterization

Scanning electron microscopy (SEM) was performed using a Zeiss Ultra Plus field emission scanning electron microscope. Surface area measurements were made using the BET method on a Quantachrome Nova 4200e. Mechanical testing was performed with a Zwick tensile tester Z100 using a 100 N load cell with a crosshead speed of 0.5 mm min^{-1}. For each sample, mechanical tests were made on five strips, and the mean and standard deviation of the relevant mechanical parameters calculated. The response of the materials to target gases was recorded by measuring the current change for a fixed applied voltage, in an enclosed cell through which the gas flowed at a rate of 0.4 l/min. Raman spectroscopy was carried out using an Avalon 785 nm Raman spectrometer at 2 cm^{-1} resolution, 3 s per scan and 10–20 collections. A 785 nm laser line was used as it can detect both doped and dedoped features in PAni.

3. Results and discussion

Through controlling the volume and quality of both CNT and PAni nanofiber dispersions used during preparation the properties of the composite films were easily controlled and reproduced. Film thicknesses were controlled in this manner, and composites with thicknesses ranging from 17 μm to 69 μm were prepared (all diameters were kept constant at 47 mm,

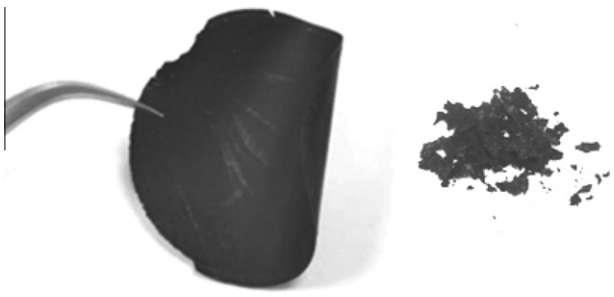

Fig. 1 – Photo of free-standing composite (left) PAni film removed from filter paper (right).

Fig. 1). The density of the films was measured and found to have an average value of 510 kg/m^3. They are extremely porous and contain 67% free volume. The CNTs act as a scaffold to reinforce the mechanical integrity of PAni nanofiber macrostructure, enabling films to be handled and cut with ease. Similar films of PAni nanofibers alone could not be prepared as once PAni fibers dry the film becomes extremely brittle, cracks and crumbles back into a powder if removed from the filter paper support, Fig. 1. Above a ratio of 50% PAni the films were no longer mechanically stable and so this mass fraction was chosen for detailed study. In order to have some comparable reference material, PAni nanofiber films, of various thicknesses, were prepared by filtration onto PVDF filter papers. As thicker PAni films crack, films with a thickness of 100 nm to 3.3 μm were prepared. It was not possible to peel these from the filter paper, and so they were tested while supported. A free standing CNT only film was also prepared.

Electron microscopy images of a CNT only film, a supported film of PAni, and a composite film are shown in Fig. 2. In Fig 2A the CNTs are porously arranged in bundles with diameters of ~10 nm. In Fig. 2B the PAni nanofibers are tangled together, their diameters ranging from 30 to 50 nm (see inset). The structure of the composite (Fig. 2C) shows clearly its porous nature. The thinner web-like tubes that appear slightly brighter (due to their higher conductivity) are the CNTs, the thicker fibers spread homogeneously among them are the PAni nanofibers. The surface area of the composite film, measured by the BET method was determined to be 371 m^2/g. Kaner and co-workers measured the surface area of PAni nanofibers alone to be 41.2 m^2/g [16]. We can assume that the increased value for the composite is due to the highly porous arrangement of the CNTs. CNT bucky papers have been reported to have surface areas up to 470 m^2/g [52].

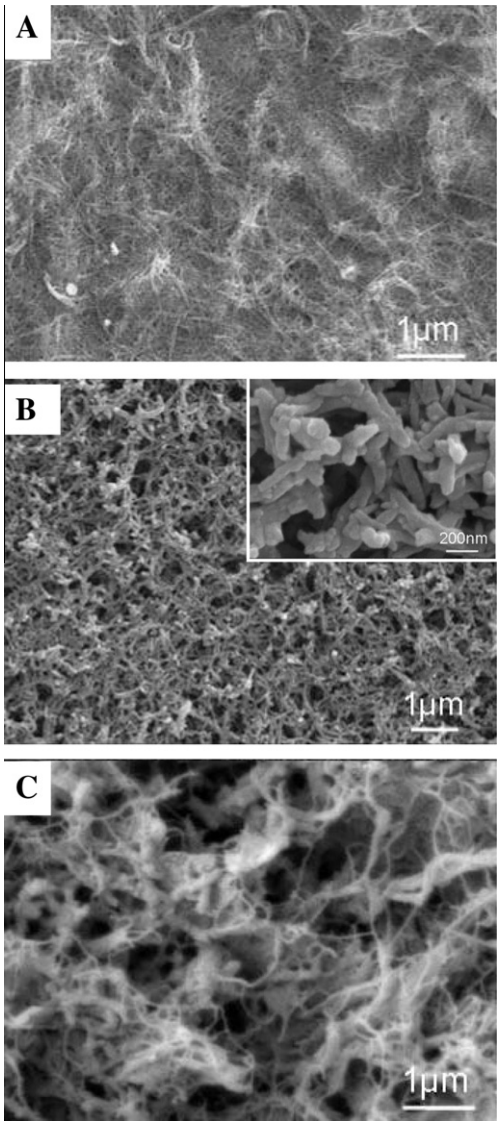

Fig. 2 – FESEM of (A) CNT buckypaper, (B) PAni nanofibers and (C) surface of composite material.

Tensile tests were carried out on the free-standing films, and their mechanical properties were found to be slightly improved by the presence of the PAni nanofibers (Table 1). The Young's modulus (or stiffness) of the composite was ~2 GPa, almost double that of the CNT only film. The strength of CNT–PAni films was also found to be greater than those of the CNT only films, at 9.9 MPa and 6.4 MPa, respectively. The mechanical properties of reference PAni films however could not be measured due to their extreme brittleness. The increase in the mechanical properties of the composite films may seem surprising as the PAni fibers themselves show no mechanical integrity in film form. It may however be a result of the difference in densities between the two types of film. The density of the CNT film is 380 kg/m^3 whereas the composite film is denser at 510 kg/m^3. This higher density may enable an increased number of physical crosslinks within the composite which has been show previously to contribute to improved mechanical properties [27].

As PAni is known to be a highly responsive active material, films were subsequently exposed to a range of target gases and the resulting change in their conductivity recorded. Fig. 3 shows the response of PAni–CNT composites to 100 ppm hydrogen sulfide, carbon dioxide and ammonia, in terms of change in conductivity relative to original conductivity ($\Delta\sigma/\sigma_0$%). Reference films of PAni and CNTs were also tested for comparison.

Of all the targets tested, the composite responds most strongly to NH_3 with a relative change in conductivity ($\Delta\sigma/\sigma_0$) of 29% when exposed to 100 ppm NH_3. This compares well with other PAni composite responses for ammonia found in the literature e.g., 18% $\Delta R/R_0$ [53] or an optical transmittance change 5% [54]. A much higher $\Delta R/R_0$ response of 400% to NH_3 has also been reported [55] but this study failed to demonstrate a steady-state signal recovery behavior during extended testing.

The sensing performance of composite films may be attributed to a combination of electrical resistance changes due to doping/dedoping of the PAni, and to a lesser extent charge transfer between the electron-donating NH_3 and the SWNTs. As the composite is comprised of 50% w/w PAni nanofibers, with the rest being CNTs, the response is less than that of the supported PAni only film. The decrease in sensitivity compared to the PAni only film may be due to the smaller amount of PAni present in composite films of equivalent scale, and the mixed PAni–CNT conduction mechanisms.

Table 1 – Mechanical properties of PAni–CNT composites, in comparison to CNT buckypapers.

	Young's modulus (GPa)	Strength at break (MPa)	Strain at break	Toughness (kJ/m^3)
CNT	1.1 ± 0.2	6.4 ± 1.8	0.006 ± 0.001	20 ± 9
Composite	1.9 ± 0.7	9.9 ± 3.4	0.006 ± 0.002	50 ± 25

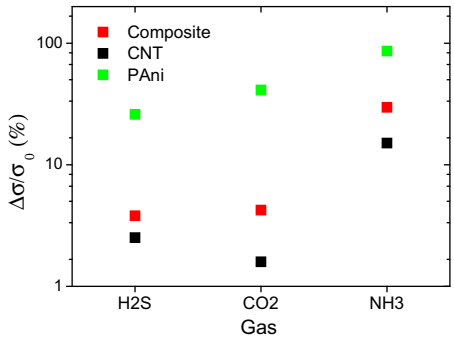

Fig. 3 – Relative response of composite, CNT film and supported PAni film to 100 ppm of H_2S, CO_2 and NH_3.

The CNT-only films register the lowest response in all cases. Gas sensors based on pristine SWNTs usually display poor sensitivity due to the lack of a specific mode of interaction between SWNTs and the target analyte [37]. Functionalization or defects on CNTs can contribute to improved sensing abilities; however the SWNTs used in this study are unfunctionalized and relatively defect free.

As the composite responds most strongly to ammonia (Fig. 3), its response/recovery behavior for this target was investigated further. Ammonia (NH_3) is found throughout the natural environment in the air, soil, water, and also in plants and animals including humans. High levels of NH_3 can result in irritation to the skin, eyes, and respiratory tracts of humans. Exposure to 300 ppm is immediately dangerous to both life and health. Ammonia is also flammable at concentrations of approximately 15–28% by volume in air. An acceptable 8 h exposure limit at 25 ppm and a short-term (15 min) exposure level at 35 ppm by volume has been set as the threshold limit value for NH_3 [56].

In order to investigate the composite's ability to respond and recover after repeated exposure to ammonia, the composite was exposed to alternate flows of 10 ppm NH_3 and air (Fig. 4) for an extended amount of time. NH_3 is a basic gas and therefore acts to dedope the composite causing a drop in conductivity; samples were purged with air to re-establish the baseline conductivity. For comparison, a carbon nanotube only film (Fig. SI3) and a selection of supported films of PAni nanofibers were treated in an identical manner. Data for the 1 μm and the 3.3 μm thick film, which showed the most significant and lasting response, is shown in Fig. 4. The carbon nanotube film, the least sensitive from initial tests in Fig. 3 registered a very low $\Delta\sigma/\sigma_0$ value of 0.17%. This allows us to attribute the response of the composite to the PAni nanofibers. In the case of the composite, the magnitude of response, $\Delta\sigma/\sigma_0$, was steady at 6%. This value is less than the 35% response of a 3.3 μm PAni film. The main point to note is that the composite responds and recovers steadily over the entire testing period of 18 days (41 h total testing time), with no observable degradation. The composite was not heated or treated in anyway and was stored in an ambient environment between tests.

In contrast, the response of the 3.3 μm PAni-only film quickly degrades from 35% on day one to 14% on day two, ceasing to respond by day three (total responsive lifetime was <7 h). Even more dramatic response degradation was observed for the 1 μm PAni film, which stopped responding after just 4 h, Fig. 4.

The effect of thickness on composite response was also investigated (Fig. SI1). Samples of various thicknesses (17–69 μm) were exposed to 10 ppm of NH_3, followed by air for 20 min intervals over 3 h. All films showed a steady response and recovery. The magnitude of all composite responses was reasonably similar measuring between 5% and 9%. This is in good agreement with work done by Virji et al. on PAni nanofiber thin films, where they report response to be thickness independent [18].

The initial response of the films in Fig. 4 is to be expected as cycled exposure to ammonia gas and air causes PAni to switch reversibly between a doped emeraldine salt form, and a dedoped emeraldine base form, the chemical structure of each is shown in Fig. SI2. This doping/dedoping is accompanied by a change in conductivity. In its conductive form PAni is protonated, which affects conjugation along the polymer backbone resulting in two positive charges per monomer unit (hence bipolaron formation). In this state charge transfer can occur along the polymer chain. Upon exposure to a base, such as ammonia, the PAni is deprotonated. Charge transfer can no longer occur and PAni is therefore insulating. This effect is reversible and PAni can switch easily between its doped and dedoped form, depending on its immediate environment. Short term redox stability is however a limitation for unmodified PAni [57], and in Fig. 4 we see that our PAni nanofiber films cease to respond after less than 8 h of testing.

As the doping/dedoping of PAni is also accompanied by a change in the optical properties of the material, the redox state of the PAni nanofibers in both the composite and the supported PAni films after testing was monitored using Raman spectroscopy [58]. In Fig. 5A PAni dispersions have been exposed to acidic and basic environments to illustrate their characteristic spectra in each state. In low pH environments, the polymer exists in the doped, conductive state with signature bands present between 1300 and 1400 cm^{-1} and 1500–1550 cm^{-1}. Increasing the pH, for example using KOH, causes a change in the bonding structure of the material and a strong peak at 1400–1500 cm^{-1} emerges, while those previously mentioned for the doped state disappear. In particular, peaks at 1340 cm^{-1} can be assigned to a C–N$^{\cdot+}$ polaron stretch [33,59] and peaks at ~1460 cm^{-1} are characteristic of C=N quinoid groups.

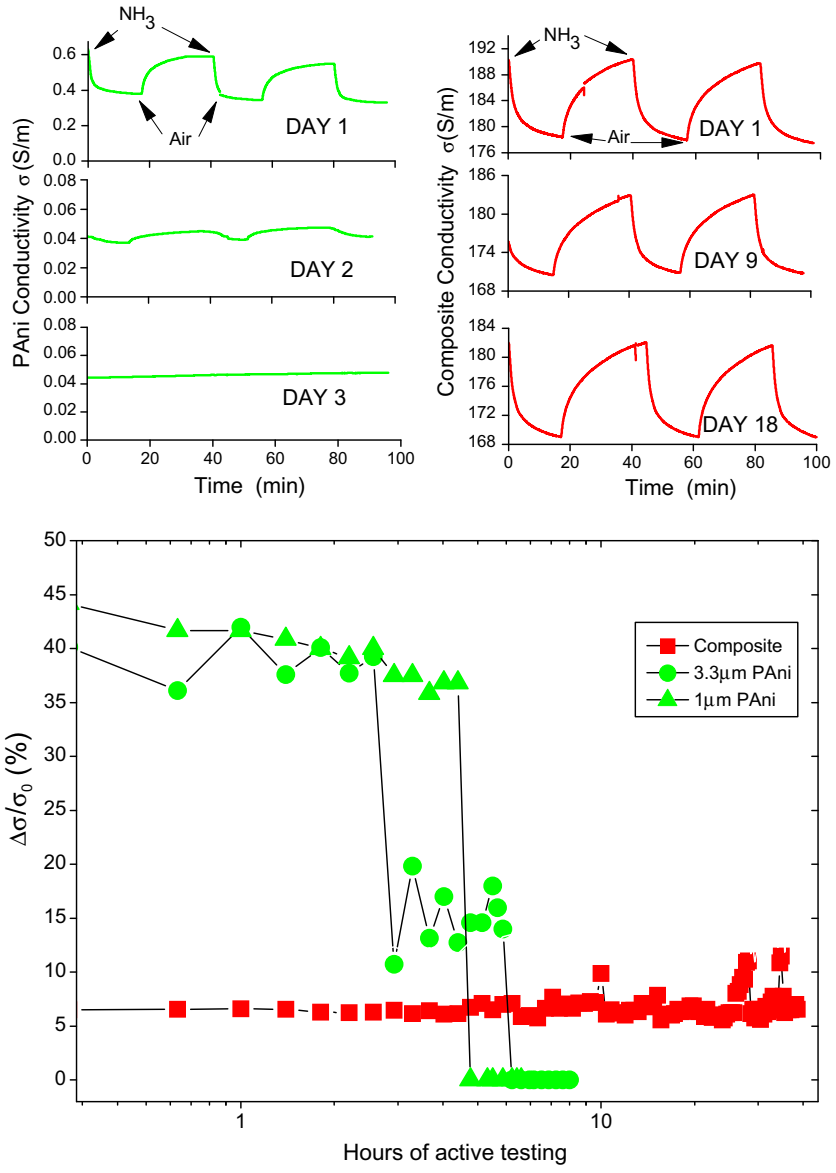

Fig. 4 – Top left, response of PAni film repeatedly exposed to 10 ppm NH_3 and flushed with air at controlled intervals. Top right, response of composite film repeatedly exposed to 10 ppm NH_3 and flushed with air at controlled intervals. Bottom, relative change in conductivity of composite and two PAni only films to exposure to NH_3 flowed by air for several hours over 18 days.

The Raman spectra for a pristine PAni nanofiber film shows the material to be in an intermediate state between fully doped and dedoped prior to testing, Fig. 5C. Spectra of the PAni films after testing however show that the material is completely dedoped, reflected by a clear peak at 1460 cm^{-1}. This is to be expected as the film had completely stopped ceased responding to ammonia.

The PAni–CNT composites were also examined both after forced doping/dedoping (using concentrated HCl and KOH, respectively), and also after prolonged exposure to cycled ammonia/air (same sample as in Fig. 4). Spectra for the forcibly doped/dedoped composites show characteristic bands for the respective states. The composite after 18 days of ammonia exposure however does not show a dedoped band and is still responsive to the target gas (Fig. 5). No peak is present at 1460 cm^{-1} suggesting that the PAni component of the composite has remained in its doped state (Fig. 5B). Therefore, we can say that by introducing CNTs to a PAni nanofiber film it is possible to improve the response/recovery lifetime of PAni, making it is less likely to transition fully into the dedoped state.

The mechanism by which CNTs extend the switching lifetime of PAni is not fully understood. CNTs are known to be good electron acceptors; conversely PAni is known to be a good electron donor. Therefore, it is reasonable to expect that CNTs and PAni should interact favorably together. In fact it has been reported that CNTs can act as PAni dopants, interacting with both N–H bonding and also quinoid rings on the PAni backbone to increase PAni conductivity [60]. Site-selective interactions between the quinoid ring on the PAni

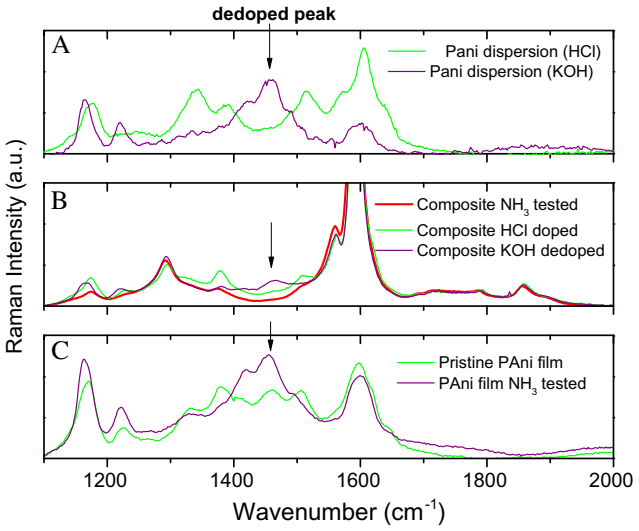

Fig. 5 – Raman spectra of (A) PAni dispersions, (B) composite films and (C) supported PAni films.

backbone and MWNTs have been reported to facilitate charge transfer between the two components [31]. Where PAni is HCl doped the CNTs actually compete with Cl^- dopant ions, suggesting that CNTs interactions are the more favored. CNTs are also a large surface area one-dimensional conductors and it is feasible that they may provide an electron transfer path between PAni nanofibers. Due to their limited size, molecular dopants such as HCl are unable to facilitate electron mobility in a similar manner.

4. Conclusion

Due to their responsive nature and high surface area, much research has been done on PAni nanofibers for sensing applications. We have demonstrated a method whereby CNTs can be used to extend the response/recovery lifetime of PAni in its nanofiber form as a porous free-standing film. The composite films have improved mechanical and electrical properties when compared with PAni nanofibers alone. Investigation of composite lifetime shows significantly improved performance. The mechanism by which the lifetime of the PAni is extended is not yet fully clear, but appears to be related to the fact that CNTs can act as a dopant for the polymer. Further studies are required to fully understand the exact interaction mechanism between the two nanomaterials. It is envisaged that the composite material described should be useful for application in autonomous sensor devices.

Acknowledgment

Fiona Blighe thanks the Irish Research Council for Science, Engineering and Technology (IRCSET) for financial support (IRCSET EMPOWER Post-Doctoral Grant).

Appendix A. Supplementary data

Supplementary data associated with this article can be found, in the online version, at doi:10.1016/j.carbon.2011.10.022.

REFERENCES

[1] Lahiff E, Woods T, Blau W, Wallace G. G, Diamond D. Synthesis and characterisation of controllably functionalised polyaniline nanofibres. Synth Met 159(7–8):741–748.
[2] Janata J, Josowicz M. Conducting polymers in electronic chemical sensors. Nat Mater 2003;2(1):19–24.
[3] Baughman RH. Conducting polymer artificial muscles. Synth Met 1996;78(3):339–53.
[4] Frackowiak E, Khomenko V, Jurewicz K, Lota K, Béguin F. Supercapacitors based on conducting polymers/nanotubes composites. J Power Sources 2006;153(2):413–8.
[5] Novak P, Muller K, Santhanam KSV, Haas O. Electrochemically active polymers for rechargeable batteries. Chem Rev 1997;97(1):207–82.
[6] Spinks GM, Mottaghitalab V, Bahrami-Samani M, Whitten PG, Wallace GG. Carbon-nanotube-reinforced polyaniline fibers for high-strength artificial muscles. Adv Mater 2006;18(5):637–40.
[7] Yang Y, Heeger AJ. Polyaniline as a transparent electrode for polymer light-emitting diodes: lower operating voltage and higher efficiency. Appl Phys Lett 1994;64(10):1245–7.
[8] Gerard M, Chaubey A, Malhotra BD. Application of conducting polymers to biosensors. Biosens Bioelectron 2002;17(5):345–59.
[9] Peng H, Zhang L, Soeller C, Travas-Sejdic J. Conducting polymers for electrochemical DNA sensing. Biomaterials 2009;30(11):2132–48.
[10] Wang J, Chan S, Carlson RR, Luo Y, Ge G, Ries RS, et al. Electrochemically fabricated polyaniline nanoframework electrode junctions that function as resistive sensors. Nano Lett 2004;4(9):1693–7.
[11] Crean C, Lahiff E, Gilmartin N, Diamond D, O'Kennedy R. Polyaniline nanofibres as templates for the covalent immobilisation of biomolecules. Synthetic Metals;161 (3-4):285-92. doi:10.1016/j.synthmet.2010.11.037.
[12] MacDiarmid AG. "Synthetic metals": a novel role for organic polymers (Nobel lecture). Angew Chem Int Ed 2001;40(14):2581–90.
[13] Moo Lee Y, Yong Nam S, Yong Ha S. Pervaporation of water/isopropanol mixtures through polyaniline membranes doped with poly(acrylic acid). J Membr Sci 1999;159(1–2):41–6.
[14] Zhou J, Tzamalis G, Zaidi N, Comfort N, Monkman A. Effect of thermal aging on electrical conductivity of the 2-acrylamido-2-methyl-1-propanesulfonic acid-doped polyaniline fiber. J Appl Polym Sci 2001;79(13):2503–8.
[15] Crowley K, O'Malley E, Morrin A, Smyth MR, Killard AJ. An aqueous ammonia sensor based on an inkjet-printed polyaniline nanoparticle-modified electrode. Analyst 2008;133(3):391–9.
[16] Huang JX, Virji S, Weiller BH, Kaner RB. Polyaniline nanofibers: facile synthesis and chemical sensors. J Am Chem Soc 2003;125(2):314–5.
[17] Virji S, Fowler JD, Baker CO, Huang JX, Kaner RB, Weiller BH. Polyaniline manofiber composites with metal salts: chemical sensors for hydrogen sulfide. Small 2005;1(6):624–7.
[18] Virji S, Huang JX, Kaner RB, Weiller BH. Polyaniline nanofiber gas sensors: examination of response mechanisms. Nano Lett 2004;4(3):491–6.
[19] Virji S, Kaner RB, Weiller BH. Hydrazine detection by polyaniline using fluorinated alcohol additives. Chem Mater 2005;17(5):1256–60.
[20] Virji S, Kaner RB, Weiller BH. Hydrogen sensors based on conductivity changes in polyaniline nanofibers. J Phys Chem B 2006;110(44):22266–70.
[21] Huang JX, Kaner RB. A general chemical route to polyaniline nanofibers. J Am Chem Soc 2004;126(3):851–5.

[22] Huang JX, Kaner RB. The intrinsic nanofibrillar morphology of polyaniline. Chem Commun 2006(4):367–76.
[23] Min G. Conducting polymers and their applications in the film industry – polyaniline/polyimide blended films. Synth Met 1999;102(1–3):1163–6.
[24] Liab D, Kaner RB. How nucleation affects the aggregation of nanoparticles. J Mater Chem 2007;17:2279–82.
[25] Baughman RH, Zakhidov AA, de Heer WA. Carbon nanotubes – the route toward applications. Science 2002;297(5582):787–92.
[26] Coleman JN, Khan U, Gun'ko YK. Mechanical reinforcement of polymers using carbon nanotubes. Adv Mater 2006;18(6):689–706.
[27] Blighe FM, Lyons PE, De S, Blau WJ, Coleman JN. On the factors controlling the mechanical properties of nanotube films. Carbon 2008;46(1):41–7.
[28] Lahiff E, Lynam C, Gilmartin N, O'Kennedy R, Diamond D. The increasing importance of carbon nanotubes and nanostructured conducting polymers in biosensors. Anal Bioanal Chem 2010;398(4):1575–89.
[29] Coleman JN, Khan U, Blau WJ, Gun'ko YK. Small but strong: a review of the mechanical properties of carbon nanotube–polymer composites. Carbon 2006;44(9):1624–52.
[30] Ali SR, Ma Y, Parajuli RR, Balogun Y, Lai WYC, He H. A nonoxidative sensor based on a self-doped polyaniline/carbon nanotube composite for sensitive and selective detection of the neurotransmitter dopamine. Anal Chem 2007;79(6):2583–7.
[31] Cochet M, Maser WK, Benito AM, Callejas MA, Martínez MT, Benoit J-M, et al. Synthesis of a new polyaniline/nanotube composite: in-situ polymerisation and charge transfer through site-selective interaction. Chem Commun 2001:1450–1.
[32] Feng W, Bai XD, Lian YQ, Liang J, Wang XG, Yoshino K. Well-aligned polyaniline/carbon-nanotube composite films grown by in-situ aniline polymerization. Carbon 2003;41(8):1551–7.
[33] He L, Jia Y, Meng F, Li M, Liu J. Gas sensors for ammonia detection based on polyaniline-coated multi-wall carbon nanotubes. Mater Sci Eng B 2009;163(2):76–81.
[34] Huang J-E, Li X-H, Xu J-C, Li H-L. Well-dispersed single-walled carbon nanotube/polyaniline composite films. Carbon 2003;41(14):2731–6.
[35] Khomenko V, Frackowiak E, Béguin F. Determination of the specific capacitance of conducting polymer/nanotubes composite electrodes using different cell configurations. Electrochim Acta 2005;50(12):2499–506.
[36] Konyushenko EN, Stejskal J, Trchová M, Hradil J, Kovárová J, Prokes J, et al. Multi-wall carbon nanotubes coated with polyaniline. Polymer 2006;47(16):5715–23.
[37] Lim J-H, Phiboolsirichit N, Mubeen S, Deshusses MA, Mulchandani A, Myung NV. Electrical and gas sensing properties of polyaniline functionalized single-walled carbon nanotubes. Nanotechnology 2010;21(7):075502.
[38] Wu M, Snook GA, Gupta V, Shaffer M, Fray DJ, Chen GZ. Electrochemical fabrication and capacitance of composite films of carbon nanotubes and polyaniline. J Mater Chem 2005:2297–303.
[39] Wu T-M, Lin Y-W. Doped polyaniline/multi-walled carbon nanotube composites: preparation, characterization and properties. Polymer 2006;47(10):3576–82.
[40] Wu T-M, Lin Y-W, Liao C-S. Preparation and characterization of polyaniline/multi-walled carbon nanotube composites. Carbon 2005;43(4):734–40.
[41] Sainz R et al. A soluble and highly functional polyaniline–carbon nanotube composite. Nanotechnology 2005;16(5):S150.
[42] Yan X-b, Han Z-j, Yang Y, Tay B-k. Fabrication of carbon nanotube–polyaniline composites via electrostatic adsorption in aqueous colloids. J Phys Chem C 2007;111(11):4125–31.
[43] Meng C, Liu C, Fan S. Flexible carbon nanotube/polyaniline paper-like films and their enhanced electrochemical properties. Electrochem Commun 2009;11:186–9.
[44] Blighe F, Blau WJ, Coleman JN. Towards tough, yet stiff, composites by filling an elastomer with single walled carbon nanotubes. Nanotechnology 2008;19:415709.
[45] Blighe FM, Hernandez YR, Blau WJ, Coleman JN. Observation of percolation-like scaling – far from the percolation threshold – in high volume fraction, high conductivity polymer-nanotube composite films. Adv Mater 2007;19(24):4443–7.
[46] Li D, Huang J, Kaner RB. Polyaniline nanofibers: a unique polymer nanostructure for versatile applications. Acc Chem Res 2008;42(1):135–45.
[47] Shane DB, Valeria N, Philip VS, Silvia G, Zhenyu S, Alan HW, et al. Towards solutions of single-walled carbon nanotubes in common solvents. Adv Mater 2008;20(10):1876–81.
[48] Sun Z, Nicolosi V, Rickard D, Bergin SD, Aherne D, Coleman JN. Quantitative evaluation of surfactant-stabilized single-walled carbon nanotubes: dispersion quality and its correlation with zeta potential. J Phys Chem C 2008;112(29):10692–9.
[49] White B, Banerjee S, O'Brien S, Turro NJ, Herman IP. Zeta-potential measurements of surfactant-wrapped individual single-walled carbon nanotubes. J Phys Chem C 2007;111(37):13684–90.
[50] Sun J, Gao L. Development of a dispersion process for carbon nanotubes in ceramic matrix by heterocoagulation. Carbon 2003;41(5):1063–8.
[51] Bergin SD, Nicolosi V, Streich PV, Giordani S, Sun Z, Windle AH, et al. Towards solutions of single-walled carbon nanotubes in common solvents. Adv Mater 2008;20(10):1876–81.
[52] Izadi-Najafabadi A, Yamada T, Futaba DN, Yudasaka M, Takagi H, Hatori H, et al. High-power supercapacitor electrodes from single-walled carbon nanohorn/nanotube composite. ACS Nano 5(2):811–9. doi:10.1021/nn1017457.
[53] Yoo K-P, Kwon K-H, Min N-K, Lee MJ, Lee CJ. Effects of O_2 plasma treatment on NH_3 sensing characteristics of multiwall carbon nanotube/polyaniline composite films. Sens Actuators B 2009;143(1):333–40.
[54] Nicho ME, Trejo M, García-Valenzuela A, Saniger JM, Palacios J, Hu H. Polyaniline composite coatings interrogated by a nulling optical-transmittance bridge for sensing low concentrations of ammonia gas. Sens Actuators B 2001;76(1–3):18–24.
[55] Tai H, Jiang Y, Xie G, Yu J, Chen X. Fabrication and gas sensitivity of polyaniline–titanium dioxide nanocomposite thin film. Sens Actuators B 2007;125(2):644–50.
[56] Blighe FM, Young K, Vilatela JJ, Windle AH, Kinloch IA, Deng L, et al. The effect of nanotube content and orientation on the mechanical properties of polymer–nanotube composite fibers: separating intrinsic reinforcement from orientational effects. Adv Funct Mater 21(2):364-71. doi:10.1002/adfm.201000940.
[57] Guimard NK, Gomez N, Schmidt CE. Conducting polymers in biomedical engineering. Prog Polym Sci; 32 (8-9):876-921. doi:10.1016/j.progpolymsci.2007.05.012.
[58] Ohira M, Sakai T, Takeuchi M, Kobayashi Y, Tsuji M. Raman and infrared spectra of polyaniline. Synth Met 1987;18(1–3):347–52.
[59] Mazeikiene R, Statino A, Kuodis Z, Niaura G, Malinauskas A. In situ Raman spectroelectrochemical study of self-doped polyaniline degradation kinetics. Electrochem Commun 2006;8(7):1082–6.
[60] Zengin H, Zhou W, Jin J, Czerw R, Smith Jr DW, Echegoyen L, et al. Carbon nanotube doped polyaniline. Adv Mater 2002;14(20):1480–3.